Fully Valley-Polarized Electron Beams in Graphene

J. L. Garcia-Pomar,* A. Cortijo, and M. Nieto-Vesperinas
Instituto de Ciencia de Materiales de Madrid, CSIC, Cantoblanco, Madrid E-28049, Spain
(Received 2 October 2007; published 10 June 2008)

We propose a device to break the valley degeneracy in graphene and produce fully valley-polarized currents that can be either split or collimated to a high degree in a experimentally controllable way. The proposal combines two recent seminal ideas: negative refraction and the concept of valleytronics in graphene. The key new ingredient lies in the use of the specular shape of the Fermi surface of the two valleys when a high electronic density is induced by a gate voltage (trigonal warping). By changing the gate voltage in a *n-p-n* junction of a graphene transistor, the device can be used as a valley beam splitter, where each of the beams belong to a different valley, or as a collimator. The result is demonstrated through an optical analogy with two-dimensional photonic crystals.

DOI: 10.1103/PhysRevLett.100.236801 PACS numbers: 73.23.Ad, 42.70.Qs, 42.79.Fm, 85.75.−d

Since its recent synthesis [1], a single layer of neutral graphite (graphene) has been a fruitful system of ideas coming from varied areas of physics. Because of the special geometry of the honeycomb lattice, the band structure of graphene is such that its valence and conduction band touch each other in six Fermi points where the dispersion relation is linear [2]. Two of these points are inequivalent and constitute the Fermi surface of the neutral material. In the absence of short range interactions, the two points remain degenerate and constitute the so-called valley degree of freedom. Most of the excitement about graphene stems from the very low energy region where the dispersion is linear and the elementary excitations are described by massless Dirac spinors, a relativistic description for a condensed matter system [3,4]. We will notice, however, that, at intermediate energies of the order of 0.6–0.7 eV easily accessible with a gate voltage, the constant energy curves acquire a nontrivial distortion [5], trigonal warping (TW), which is different in the two valleys. This will be the key ingredient to a substantial improvement of the experimental realization of a valley splitting in graphene.

In a recent publication [6], it has been suggested that the valley degree of freedom could be used to carry information in electronic devices if a controllable way is found to produce valley polarization. A device was suggested based on a point contact junction between graphene ribbons with special termination (zigzag edges). Previously, in another seminal paper [7], the Fermi surface and the dispersion relation at low energies were used to suggest the possibility of focusing electron beams by a *p-n* junction, the *n-p-n* junction acting as a lens. A beam splitter would be obtained by giving a triangular shape to the *p* region in the *n-p-n* junction. Both proposals require a quite precise tailoring of the graphene samples that hardens their experimental realization.

In this work, we combine the two former ideas and propose a very simple way to construct a beam splitter where each of the electronic beams is fully polarized in the valley quantum number. In what follows, we will describe the mechanism based on a *n-p-n* junction in detail and show how it can be tested in an optical device. As we show, the present mechanism allows us to obtain fully polarized currents in graphene samples of arbitrary shapes. We will start by reviewing the way in which the transmission of electrons through the *p-n* interface resemble the optical refraction at the surface of metamaterials with a negative refractive index as suggested in Ref. [7]. Then we address the role played by the TW distortion and the relative orientations of the *p* and *n* regions.

In the tight-binding approximation of the low energy band structure for graphene, the dispersion relation including both the Dirac and the TW terms is

$$E_s(\mathbf{k}) = \pm\hbar v_F\sqrt{k^2 + \frac{a^2}{16}k^4 + \frac{a}{2}s(k_x^3 - 3k_xk_y^2)}, \qquad (1)$$

where v_F is the Fermi velocity, a is the lattice constant, and $k^2 = k_x^2 + k_y^2$. The parameter $s = \pm 1$ refers to the two valleys.

The average current moving through the sample is $\langle \mathbf{J}_s \rangle = \frac{e}{\hbar}|t_s|^2\mathbf{v}_{g,s}$, where t_s represents the transmission coefficient and $\mathbf{v}_{g,s}$ stands for the group velocity in each valley. When the TW term is considered, $\mathbf{v}_{g,s}$ is

$$\mathbf{v}_{g,s} = \frac{1}{\hbar}\nabla_{\mathbf{k}}E_s(\mathbf{k}) = \pm\frac{v_F^2}{2E_s(\mathbf{k})}\left[\left(2 + \frac{a^2}{4}k^2\right)\mathbf{k} + \frac{a}{2}s\mathbf{F}\right], \qquad (2)$$

where $\mathbf{F} = (3k_x^2 - 3k_y^2, -6k_xk_y)$. We notice that the presence of the TW term does not essentially alter the value $|t_s|^2$ of the *p-n* junction [8,9] that has almost the same shape for both valleys. The major role in the different behavior of $\langle \mathbf{J}_s \rangle$ in the two valleys is played by the group velocity $\mathbf{v}_{g,s}$ that explicitly depends on s. As mentioned in Ref. [7], a *p-n* junction in graphene has a photonic analogy with an optical system composed of two effective media with opposite signs of their refractive index. In optical material slabs with a negative refractive index, Snell's

law leads to the phenomenon of light focusing [10,11]. A similar behavior was proposed for the electrons in graphene. If the Fermi level is chosen such that the conduction band (for which the group velocity $\mathbf{v}_g$ points *out towards* the energy surface), on one side of the junction, is connected to the valence band on the other side (where $\mathbf{v}_g$ now points *in towards* the energy surface), the system behaves as the electrical counterpart of a Veselago lens [10]. In the device of Ref. [7], the p and n regions were adjusted so that the Fermi surface had the same—almost circular—shape, and then all-angle negative refraction is obtained.

The novelty of our proposal lies in two facts. First, the TW distortion is different in the two valleys, and second, the refraction in the junction determined by the parallel momentum conservation depends on the shape of the border: The incident beam comes from the n region whose Fermi surface is a small circle. Depending on the orientation of the interface (zigzag or armchair), the straight current impinges on regions of very different curvature of the trigonal distorted Fermi surface of the p region. Figure 1 illustrates these aspects and our proposal. We show a field effect n-p^+ device in graphene. Figures 1(a) and 1(b) show the two limiting cases for the relative orientations between the deposited gate and the n region. They are (a) zigzag and (b) armchair junctions. Because of the symmetry of the honeycomb lattice, all of the possible orientations lie between these two limiting cases.

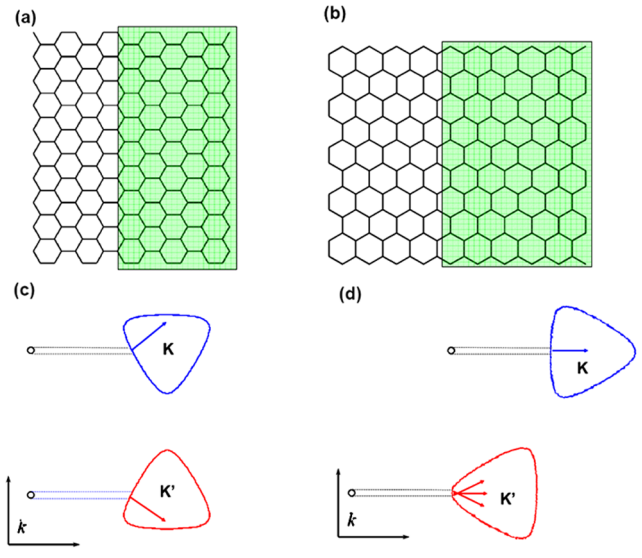

FIG. 1 (color online). (a),(b): The two limiting cases for the deposition of the gate over the graphene sample. The green area denotes the region doped with holes at energies where the TW becomes relevant. (a) Interface of the gate parallel to the zigzag orientation and (b) the armchair interface. (c),(d) represent the Fermi surface of the two valleys and the conservation of the parallel wave vector for the zigzag and armchair interface, respectively. For the zigzag junction, the refractions in the two valleys have different orientations. For the armchair interface, the transmission in one of the valleys is in the forward direction, and there is very little dispersion in the second valley.

Figures 1(c) and 1(d) show the direction of group velocity $\mathbf{v}_{g,s}$ determined by conservation of the momentum parallel to the junction interfaces for the two types of barriers. In the p^+ area, the applied gate voltage is such that the chemical potential is located at energies where the TW effect becomes relevant (according to angle-resolved photoemission spectroscopy data [12], this happens for energies of 0.6–0.7 eV). In the zigzag edge (c), the currents associated to each valley travel in different directions leading to two different currents polarized in the valley index. Figure 1(d) represents the parallel momentum conservation when the gate is oriented along the armchair direction. The current associated to one of the valleys (valley K) is fully collimated because the incident angle is almost perpendicular to the Fermi surface (which is almost a straight line). The current belonging to the other valley is more dispersed.

With these characteristics, we can design a device to achieve the realization of a valley-polarized beam splitter with a n-p-n^- junction [Figs. 2(a) and 2(b)] with the interface parallel to the zigzag orientation. In the first n zone, we introduce an electron source. In this region, the Fermi level E_F is at low energy in the conduction band, where the Fermi surface is circular and the linear Dirac regime is valid. This area is separated from a zone of low

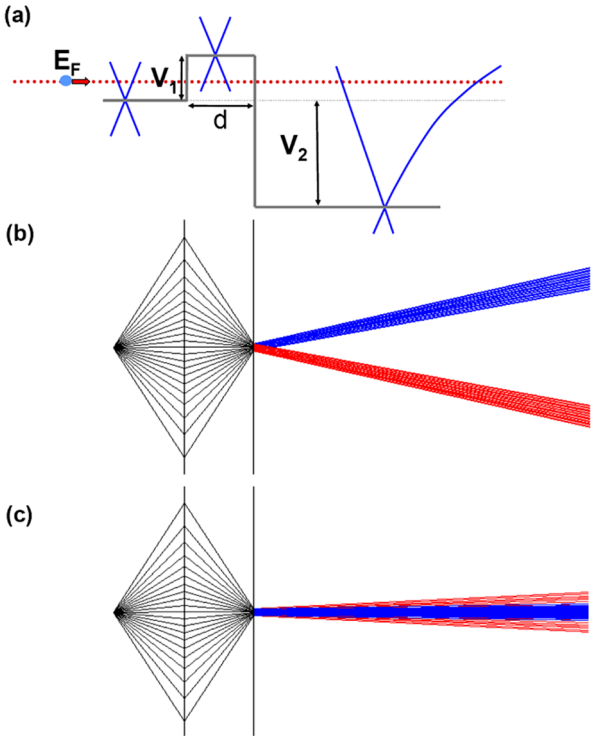

FIG. 2 (color online). (a) Potential profile of a n-p-n^- junction and schematic band structure of one valley. (b) Theoretical ray tracing of the beams coming from a point source in a junction with the interface parallel to the zigzag orientation. $E_F = 0.05$ eV, $V_1 = 0.10$ eV, and $V_2 = -1.5$ eV. The beam splitting is noticeable. (c) Armchair junction. We now obtain a collimation perpendicular to the interface.

chemical potential (p region) in the valence band, by a barrier with a potential V_1. In the interface, we have both negative refraction and focusing [7]. The last step with negative potential V_2 is placed immediately before the electron focusing in order to get a very small illuminated zone. In this way, we have narrower exit beams avoiding the formation of caustics which would appear if the position of the focus were reached before the last interface. Finally, the last region is at high voltages in the conduction band (n^- region); i.e., it has a strong TW. A polarization of valley occurs, giving rise to a beam splitting of the electronic beams belonging to different valleys [Fig. 2(b)].

A different situation occurs if the interface is parallel to the armchair orientation [Fig. 1(b)]; the beam of one valley is strongly collimated and waveguided [blue area in Fig. 2(c)] due to the flat portion of the isofrequency line. The other valley slightly disperses the beam. Because of the big difference of curvatures between the Dirac and the TW isoenergies, the allowed wave vectors $\mathbf{k}$ are situated in a zone of the TW isoline with small curvature involving a low dispersion [red area in Fig. 2(c)].

Figure 3(a) shows current versus voltage for normal transmission, observing that the beams are totally separated at moderate voltages (zero current for normal transmission), and at angle of transmission $\theta_t = 12.7°$ showing a valley-polarized peak at high voltages. A realistic transmission probability for the beam splitter is shown in Fig. 3(b). We observed that the high transmission obtained for low energies [8] is conserved when the TW term is included. The two beams were obtained for a potential $V_2 = -1.5$ eV (TW case) 25.4° apart from each other for maximum of transmission.

Let us make a comment on the possible experimental realization of the proposed device. To date, the most efficient way of identifying graphene samples is by optical contrast [13]. The peak of this contrast depends both on the thickness of the substrate and on the wavelength of the monochromatic radiation used to illuminate the sample, usually in the visible range. This peak corresponds to a thickness of 300 nm, and the values reached for the chemical potential are of the order of 0.3 eV. However, it has been proposed [14] that another maximum in the contrast appears at a thickness of 90–100 nm. With this range, it is possible to get values of the chemical potential up to 0.6 eV, just in the threshold where the TW starts to be appreciable. The effect discussed here can then be effectively observed with minor experimental changes in current samples, namely, increasing the gate voltage and decreasing the substrate thickness. In large doping, the screening is efficient and Coulomb interaction can be rescaled, so that a one-particle model (Fermi liquid) is appropriate. The electron-electron Coulomb interaction could slightly distort the isoenergy lines as was shown both experimentally [15] and theoretically [16]. However, this distortion only increases the separation of the beams. Concerning the effect of disorder in realistic samples, the quality of the valley splitter presented in this work relies mainly on the independence of the two valleys of graphene. Since the intravalley scattering translates to a spreading of both beams, the effect of polarization is still present due to the flatness of the Fermi surfaces in TW. Short range disorder mixing the two valleys [17] will decrease the efficiency of the device. A recent estimate of this effect gives an intervalley mean free path [18] of the order of the samples size (~ 1 μm); hence, the splitting should be observed in actual experiments.

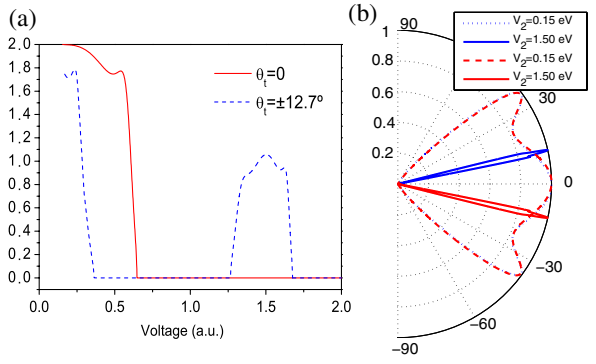

FIG. 3 (color online). (a) Current versus voltage for two transmission angle θ_t of observation. (b) Transmission probability for the K (blue lines) and K' (red lines) as a function of the output angle θ_t for different negative potentials V_2. The parameters are as follows: barrier width, $d = 100$ nm; initial energy, $E_F = 0.05$ eV; and initial potential, $V_1 = 0.14$ eV.

An optical analogy.—Control of beam propagation, collimation, and focusing in photonic crystals (PCs) is already well developed [19–22]; thus, one can assess the validity of the above analysis for graphene by putting forward its analogy with this photonic system. In fact, an optical analogy of the graphene system was previously described [23,24]. We can realize it with a 2D PC with honeycomb, kagome, or trigonal structure where the gap between the first and second bands is replaced by a Dirac point in the K point of symmetry. As an example, we have used a trigonal lattice, with parameter a_{PC}, of air cylinders of radius $r = 0.33a_{PC}$ inside a dielectric matrix with refractive index either n_1 or n_2 [Fig. 4(a)]. We notice that, in the case of the trigonal lattice, the Brillouin zone (BZ) [Fig. 4(b)] coincides with the real lattice, while in the graphene honeycomb lattice, the BZ is rotated 30° with respect to the real lattice, which implies that the zigzag and armchair situations described in graphene are exchanged in the PC. Now we cannot change the light frequency throughout the crystal like we change the chemical potential in a transistor of field effect in graphene, but we can displace the frequency position of the Dirac point in the band diagram by slightly varying the refractive index of the dielectric matrix [Fig. 4(c)]. In this way, a junction of two PCs with the same trigonal structure but with slightly different refractive index mimics the field effect transistor in graphene.

Figure 5 shows a finite element numerical simulation of the electric field modulus distribution from a light point

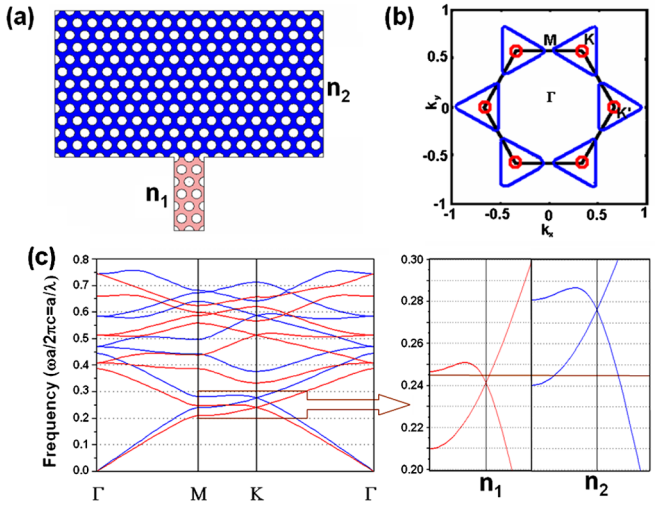

FIG. 4 (color online). (a) Geometry of the trigonal PC of air holes and optical analogy of a p-n junction in graphene. (b) Brillouin zone and isofrequency lines for the two PCs with n_1 (red circles) and with n_2 (blue triangles). (c) Band diagram for a trigonal PC described in text with refractive index $n_1 = 3.04$ (red bands) and $n_2 = 2.65$ (blue bands). The two insets show details of the zone around the K point where we observe that, for the wavelength $\lambda = 4.08a_{\mathrm{PC}}$, n_1 corresponds to the conduction band, whereas n_2 is located at the TW valence band.

source, emitting with the electric field parallel to the air hole axis at a wavelength $\lambda = 4.08a_{\mathrm{PC}}$ in a dielectric matrix with refractive index $n_1 = 3.04$ together with another PC of the same structure but a refractive index $n_2 = 2.65$ for the two limiting cases: armchair [Fig. 5(a)] and zigzag [Fig. 5(b)]. The creation of a beam splitter in the

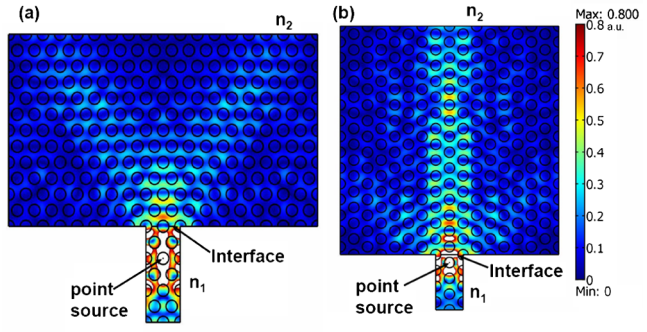

FIG. 5 (color online). Maps of the electric field modulus of a wave originated at a point source located inside a PC with matrix refractive index n_1 and propagating through another PC of dielectric matrix refractive index n_2. (a) Armchair orientation, illustrating the beam splitting of the two different valleys K and K'. (b) Zigzag orientation. We can see a collimation of the beams since the curvature in the trigonal distorted band is smaller than the one of the circular isoline in the proximity of the Dirac point. The angular dispersion is low.

latter PC for the armchair situation is illustrated by the fact that the two isofrequency curves in the K and K' points are triangles pointing in opposite directions from each other (right and left). Conversely, if we put the zigzag structure parallel to the interface, we obtain a collimation of the beams.

In summary, we have proposed an efficient way to get *valley-polarized* beams by using the TW in the graphene bands. We have shown a possible design of a beam splitter and a collimator device. This formation of valley polarization can be used as an effective information-carrying degree of freedom. Finally, we have checked the validity of these phenomena by means of an optical analogy with 2D PCs and proposed a theory of isoenergy lines as a tool to simulate these kinds of processes in graphene.

We thank M. A. H. Vozmediano, R. Aguado, and F. Guinea for useful discussions and comments. This work was supported by the Spanish DGICYT and the E.U. J. L. G.-P. acknowledges the I3P grant program. A. C. acknowledges MEC of Spain for financial support.

*jlgarcia@icmm.csic.es

[1] K. S. Novoselov *et al.*, Nature (London) **438**, 197 (2005).
[2] P. R. Wallace, Phys. Rev. **71**, 622 (1947).
[3] A. K. Geim and K. S. Novoselov, Nat. Mater. **6**, 183 (2007).
[4] A. H. Castro Neto *et al.*, arXiv:0709.1163.
[5] R. Saito, G. Dresselhaus, and M. S. Dresselhaus, Phys. Rev. B **61**, 2981 (2000).
[6] A. Rycerz, J. Tworzydło, and C. W. J. Beenakker, Nature Phys. **3**, 172 (2007).
[7] V. V. Cheianov, V. Fal'ko, and B. L. Altshuler, Science **315**, 1252 (2007).
[8] M. I. Katsnelson, K. S. Novoselov, and A. K. Geim, Nature Phys. **2**, 620 (2006).
[9] V. V. Cheianov and V. I. Fal'ko, Phys. Rev. B **74**, 041403(R) (2006).
[10] V. G. Veselago, Sov. Phys. Usp. **10**, 509 (1968).
[11] J. B. Pendry, Phys. Rev. Lett. **85**, 3966 (2000).
[12] S. Y. Zhou *et al.*, Nature Phys. **2**, 595 (2006).
[13] K. S. Novoselov *et al.*, Science **306**, 666 (2004).
[14] P. Blake *et al.*, Appl. Phys. Lett. **91**, 063124 (2007).
[15] J. L. McChesney *et al.*, arXiv:0705.3264.
[16] R. Roldan, M. Lopez-Sancho, and F. Guinea, Phys. Rev. B **77**, 115410 (2008).
[17] M. M. Fogler *et al.*, Phys. Rev. B **77**, 075420 (2008).
[18] F. V. Tikhonenko *et al.*, Phys. Rev. Lett. **100**, 056802 (2008).
[19] H. Kosaka *et al.*, Appl. Phys. Lett. **74**, 1212 (1999).
[20] M. Notomi, Phys. Rev. B **62**, 10 696 (2000).
[21] J. L. Garcia-Pomar and M. Nieto-Vesperinas, Opt. Express **13**, 7997 (2005).
[22] P. T. Rakich *et al.*, Nat. Mater. **5**, 93 (2006).
[23] F. D. M. Haldane and S. Raghu, arXiv:cond-mat/0503588.
[24] R. A. Sepkhanov, Y. B. Bazaliy, and C. W. J. Beenakker, Phys. Rev. A **75**, 063813 (2007).